J. Cent. South Univ. (2020) 27: 3821−3838
DOI: https://doi.org/10.1007/s11771-020-4473-0

Springer

Performance evaluation of nano-silica and silica fume on enhancing acid resistance of cement-based composites for underground structures

WU Lin-ping, HUANG Guang-ping, LIU Wei Victor

Department of Civil and Environmental Engineering, University of Alberta, Edmonton, Alberta T6G 2E3, Canada

Abstract: This study aims to evaluate the performance of silica fume (SF) and nano-silica (NS) on enhancing the sulfuric acid resistance of mortar mixtures. The NS and SF were added as substitutions for cement at various dosages. The cured samples were immersed in the sulfuric acid solution with a pH of 2 for 75 d. A compressive strength test and absorption and voids tests were conducted before sulfuric acid immersion. It was found that the addition of SF and NS reduced the volume of permeable voids and increased compressive strength. A thermo-gravimetric analysis was carried out to investigate the hydration of mixtures. The mixtures with SF showed a higher level of pozzolanic reaction compared with mixtures with NS. After the 75 d of immersion, the mixtures with 5% SF and 1% NS showed the best resistance against sulfuric acid because they showed the lowest mass change and length change.

Key words: acid resistance; nano-silica; silica fume; mortar

Cite this article as: WU Lin-ping, HUANG Guang-ping, LIU Wei Victor. Performance evaluation of nano-silica and silica fume on enhancing acid resistance of cement-based composites for underground structures [J]. Journal of Central South University, 2020, 27(12): 3821−3838. DOI: https://doi.org/10.1007/s11771-020-4473-0.

1 Introduction

For underground structures, a proper support system is essential to ensure their stability within the service life [1]. Of the underground support systems, cementitious material is an indispensable component for their application in grouting, shotcreting, and tunnel lining [2, 3]. For example, North American and Australian mines alone could consume 700000 m^3 of shotcrete per year [4]. However, the cementitious materials are susceptible to attacks by acids, which can be naturally generated around underground structures. For example, when sulfide-bearing rocks such as pyrites expose to air and water, the sulfur content in rocks can be oxidized, generating sulfuric acid (see equations below) [5].

$$2FeS_2+7O_2+2H_2O\rightarrow 2Fe^{2+}+4SO^{2-}{}_4+4H^+ \quad (1)$$

$$4Fe^{2+}+O_2+4H^+\rightarrow 4Fe^{3+}+2H_2O \quad (2)$$

$$4Fe^{3+}+3H_2O\rightarrow Fe(OH)_3+3H^+ \quad (3)$$

As the generated sulfuric acid contaminates groundwater, the pH of the groundwater can be reduced to as low as 2 [6]. In such acidic environments, the cement hydration products (e.g., calcium hydroxide and calcium silicate hydrate) are decomposed via the following reactions [7].

$$CH+H_2SO_4 \rightarrow C\bar{S}H \quad (4)$$

$$CSH+H_2SO_4 \rightarrow C\bar{S}H+SiO_2+H_2O \quad (5)$$

where CH is calcium hydroxide, CSH denotes calcium silicate hydrate, and $C\bar{S}H$ is the gypsum

Foundation item: Project(NSERC RGPIN-2017-05537) supported by the Natural Sciences and Engineering Research Council of Canada
Received date: 2020-05-27; **Accepted date:** 2020-09-02
Corresponding author: LIU Wei Victor, PhD, PEng, Associate Professor; Tel: +1-7802485649; E-mail: victor.liu@ualberta.ca; ORCID: https://orcid.org/0000-0002-0334-3856

($CaSO_4·2H_2O$). This decomposition process of cement hydrates damages the mechanical performance of cement-based structures, leading to a loss of structural support in underground space. Such an acid corrosion problem of underground structures has been reported in previous literature [8−14]. For instance, HAGELIA [14] reported that the generation of sulfuric acid from oxidation of pyrite reduced the pH of groundwater to 2−4 around some tunnels in Norway. This sulfuric acid attacked the sprayed concrete of road tunnels, resulting in cracking and spalling of tunnel surface after 27 years of construction. Another example of this acid attack is reported by LI et al [8] where a severe corrosion issue of cement-based structures by sulfuric acid was observed in an underground copper mine in China [8]. A thick corrosion layer was observed on the surface of the cement-based structure. At some locations of the copper mine, large deformation of tunnels was found due to this acid corrosion.

To mitigate this, cement-based materials used in underground mines should be made with high acid-resistance. By partially replacing cement with silica fume, much research has indicated that the acid resistance of concrete can be noticeably enhanced [15−17]. TORRI et al [15] investigated the acid resistance of mortar samples and found that the 10% substitution of cement with silica fume inhibited deterioration after 36 months of immersion in 2% H_2SO_4 solution. MEHTA et al [16] explored the chemical resistance of concrete mixtures and concluded that a 15% substitution of cement with silica fume demonstrated enhanced performance under 1% HCl, 1% H_2SO_4, 1% lactic acid and 5% acetic acid. WU et al [17] investigated the acid resistance of shotcrete samples and observed that a 5% cement substitution with silica fume showed the lowest mass loss and strength change after three months of exposure to sulfuric acid. The improved acid resistance has been attributed to the following two effects: 1) the pozzolanic reaction between CH and silica fume, consuming CH. CH was considered as the main component that leads to the low acid resistance of cementitious material [18]. In addition, the pozzolanic reaction generates more C-S-H, which densifies the cementitious materials and inhibits the penetration of aggressive chemicals [19, 20]. 2) The filling effect. The silica fume of a smaller size is reported to fill small pores such as those in the interfacial transition zone in the cement-based composites, which also makes the cementitious composites denser [21].

Furthermore, nanoparticles have been increasingly used in cement-based composites. Since nano-silica has a smaller particle size (1−100 nm) and higher reactivity, the pozzolanic reaction could be faster, and the filler effect could be more significant. Thus, nano-silica may have a better performance than that of silica fume in improving the acid resistance of cement-based composites. Research has been conducted to investigate the acid resistance of cementitious composites incorporating nano-silica. For instance, DIAB et al [22] immersed three grades of concrete (55, 80 and 90 MPa) in nitric acid and sulfuric acid for 360 d. They found that the inclusion of nano-silica enhanced acid resistance in terms of strength loss, weight loss and ultrasonic pulse velocity (UPV) loss. MAHDIKHANI et al [23] investigated the durability of concrete samples under sulfuric acid rain leaching. It was found that the incorporation of nano-silica reduced weight loss at all ages of leaching. In other words, acid resistance was improved by the addition of nano-silica.

However, commercial nano-silica is much more expensive than silica fume [24]. The price of commercial nano-silica can be more than 8800 US dollars per tonne [25], compared with 640 US dollars per tonne for silica fume [26]. Thus, it is economically important to compare the efficiency of nano-silica and silica fume in improving acid resistance. This can help end-users in their decision-making regarding the selection of admixtures. However, very few studies have been carried out to compare the effects of silica fume and nano-silica on the acid resistance of cementitious materials. Among the studies that have been conducted to date, contradictory results have been reported. For example, HENDI et al [27] and AMIN et al [20] found that the substitution of silica fume performed better than nano-silica in resisting sulfuric acid. However, MAHMOUD et al [28] conducted three phases of sulfuric acid immersion tests (Phase #1: pH 4.5 for 12 weeks; Phase #2: pH 1 for 12 weeks; and Phase #3: pH 0.5for 12 weeks) on concrete samples with silica fume and nano-silica. They found that only the mixtures with nano-silica

demonstrated enhanced acid resistance during Phase #2 immersion. Furthermore, contradictory results were also reported on acid resistance of silica fume containing mixtures. For example, HEWAYDE et al [29] found that concrete with silica fume exhibited no improvement in sulfuric acid resistance, which is contrary to the previous research [15, 16]. More specifically, RAHMANI et al [30] found that the sulfuric acid resistance of silica fume mixtures depended on the acidity of the immersion solution. Furthermore, other testing conditions such as wetting-drying cycles, immersion time, and the ratio of the sample surface to the acid volume were also reported to affect concrete deterioration drastically [31, 32]. Since there is currently no standard testing procedure in acid resistance evaluation, these immersion conditions could be significantly different in various studies. Thus, it is crucial to compare the effects of silica fume and nano-silica on the acid resistance of cement-based composites under the same testing procedure. In addition, it is environmentally significant to carry out this research as the silica fume is the waste from the metal and alloy production industry, while nano-silica can be extracted by processing silica fume [33]. Exploring the use of silica fume and nano-silica can help with the recycling of this industrial waste.

In this regard, the objective of this study is to evaluate the performance of silica fume and nano-silicaon enhancing the acid resistance of mortar mixtures. Silica fume and nano-silica were added to mortar mixtures to partially replace cement. The cured samples were exposed to a sulfuric acid solution with a pH of 2 for 75 d. Acid resistance was evaluated by monitoring the change in compressive strength, ultrasonic pulse velocity, mass, and length during acid immersion. This study has provided valuable results for the selection between silica fume and nano-silica in making more acid-resistant mixtures for underground structures.

2 Methodology

2.1 Materials and mix proportions

In this research, the general use (GU) type of Portland cement was used as the binding material. Table 1 lists the chemical compositions of the cement. The fine aggregate used in the mixtures was the typical sand for concrete making, with a bulk density of 1575 kg/m^3 and water absorption of 1.5%. Figure 1 presents the sieve analysis of the aggregates. The particle-size distribution of the sand was in the American Concrete Institute (ACI) grade zone #1 [34]. The silica fume, sourced from a local supplier, was added to the mortar mixture to partially replace cement at ratios of 5%, 10%, and 15%. The silica fume had a Brunauer-Emmett-Teller (BET) surface area of 2.808 m^2/g; its primary chemical composition is listed in Table 2. The nano-silica was sourced from a local supplier, and the main physical and chemical properties of it are presented in Table 3. Nano-silica was added to the mixtures as a substitution for Portland cement at ratios of 0.5%, 1.0%, 1.5% and 2.0%. In this study, the dosage selection for nano-silica and silica fume was generally based on the following reasons. First, the dosage with the best mechanical strength is included because strength is a critical parameter for the design of underground structures. Studies have reported that the optimum dosage with high strength was in the range of 0.5%−1% for nano-silica [35], and 5%−10% for silica fume [17, 36]. Second, excessive nano-silica leads to particle agglomeration that acts as defects in samples. Significant agglomeration has been reported at a dosage of ≥1.5% [37]. Thus, the max dosage of nano-silica was set at a relatively low value of 2%. Third, excessive dosage (>10%) of silica fume could lead to a reduced cement content and a significant amount of unreacted silica fume in the sample that reduces the mechanical strength [17, 38]. The mixture proportions are presented in Table 4.

Table 1 X-ray fluorescence main composition of type GU cement (mass fraction, %)

MgO	Al_2O_3	SiO_2	SO_3	CaO	Fe_2O_3
4.6	3.8	19.9	2.9	62.2	3.50

2.2 Sample preparation

Cylindrical mortar samples were cast as per ASTM C192-16a [39]. For mixtures with silica fume, the cement, fine aggregate, and silica fume were mixed in a mixing drum for 3 min, then water was added to the mixture and mixed for another 3 min. For mixtures with nano-silica, only the cement and fine aggregate were dry mixed in the mixing drum. The nano-silica was added and stirred

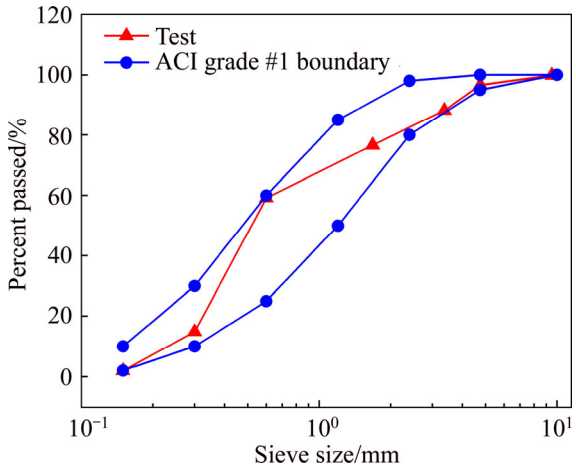

Figure 1 Sieve analysis of fine aggregates

Table 2 Primary composition of silica fume (mass fraction, %)

MgO	Al_2O_3	SiO_2	P_2O_5	SO_3	K_2O	CaO	Na_2O	Fe_2O_3
0.29	0.14	95.6	0.1	0.26	0.53	0.38	0.15	0.07

Table 3 Physical and chemical properties of nano-silica

Property	Value
Surface area (BET)/($m^2 \cdot g^{-1}$)	295
Tamped density/($g \cdot L^{-1}$)	50
Loss on drying/%	<1.5
pH value	3.7−4.5
$w(Al_2O_3)$/%	<0.03
$w(Fe_2O_3)$/%	<0.003
$w(TiO_2)$/%	<0.03
w(HCl)/%	<0.020
$w(SiO_2)$/%	>99.8

in the water to make a suspension. Then, the suspension was added to the mixing drum for another 3 min of mixing. The fully mixed wet mixture was cast into Φ50 mm×100 mm cylinder molds and stored under an ambient environment for 24 h. Then, the cylindrical samples were de-molded and stored in a moisture room with a temperature of (25±2) °C and relative humidity of 100% for 28 d.

2.3 Testing procedure

Prior to sulfuric acid immersion, some basic properties were tested on the hardened samples. First, the density, absorption, and volume of permeable voids were tested as per ASTM C642-13 [40]. For each mixture, three samples were used in the test, and then an averaged value was calculated. Second, a thermo-gravimetric analysis (TGA) was conducted to examine the hydration degree and hydration products of each mixture. To eliminate the effects of aggregate on the TGA results, cylindrical paste samples were made for each mixture (without fine aggregate). After 28 d of standard curing, two thin slices of the paste samples were cut and ground into small particles. Then, the particles were immersed in acetone for 48 h to extract free water and therefore stop the hydration reaction. After the acetone immersion, the particles were oven-dried at 60 °C for 24 h and further ground into powder smaller than <63 μm for the TGA test. For each test, (1.2±0.05) g of a sample was heated under a nitrogen atmosphere from 20 °C to 980 °C at a heating rate of 10 °C per minute. Third, the unconfined compressive strength (UCS) was monitored based on ASTM C39/C39M–18 [41]. Three samples were tested to calculate the average values.

Then, the samples were soaked in the sulfuric acid solution with a pH of 2. The ratio between acid volume to sample surface area was kept constant

Table 4 Proportioning of mixtures with silica fume and nano-silica

No.	Mixture ID	ρ(Cement)/($kg \cdot m^{-3}$)	ρ(Water)/($kg \cdot m^{-3}$)	ρ(Sand)/($kg \cdot m^{-3}$)	ρ(Admixtures)/($kg \cdot m^{-3}$)	Admixture content/%	w/c
1	Reference	493.25	221.96	1541.4	0	0	0.45
2	SF5	468.59	221.96	1541.4	24.66	5	0.45
3	SF10	443.93	221.96	1541.4	49.33	10	0.45
4	SF15	419.26	221.96	1541.4	73.99	15	0.45
5	NS0.5	490.78	221.96	1541.4	2.47	0.5	0.45
6	NS1.0	488.32	221.96	1541.4	4.93	1	0.45
7	NS1.5	485.85	221.96	1541.4	7.41	1.5	0.45
8	NS2.0	483.39	221.96	1541.4	9.88	2	0.45

with a value of 5.09 (1 L of acid per sample). Concentrated sulfuric acid was regularly (every five days) added to the immersing solution to maintain the acidity. During immersion, the UPV, mass and length of samples were monitored every 15 d. Prior to the tests, the samples were dried in the ambient environment for 24 h to eliminate the effect of moisture on mass and UPV.

After 75 d of immersion, the samples were moved out from the immersing acid for further evaluation. One sample of each mixture was cut from the middle for visual observation. The cross-section was dyed with phenolphthalein to assess the degree of corrosion visually. Then, the rest of the samples were dried and tested for the final mass, length, and UPV. After that, the samples were brushed with a steel brush to remove the corrosion layer, and the mass and length were remeasured to obtain the values after brushing. Finally, the UCS test was carried out to evaluate mechanical performance after sulfuric acid immersion.

3 Results and discussion

3.1 Properties before sulfuric acid immersion

3.1.1 Density, water absorption and permeable voids

The durability of concrete against sulfuric acid is closely related to the water absorption and volume of permeable voids of cement-based composites [42−44]. Thus, the tests for density, water absorption and volume of permeable voids were conducted for all mixtures. The results are plotted in Figures 2 and 3 for silica fume mixtures and nano-silica mixtures, respectively. It can be seen from Figure 2(a) that the incorporation of silica fume increased the bulk density from 2045.7 kg/m^3 for the reference mixture to 2071.3 kg/m^3 for the mixture with 5% silica fume. Then, the bulk density decreased with the increase of silica fume

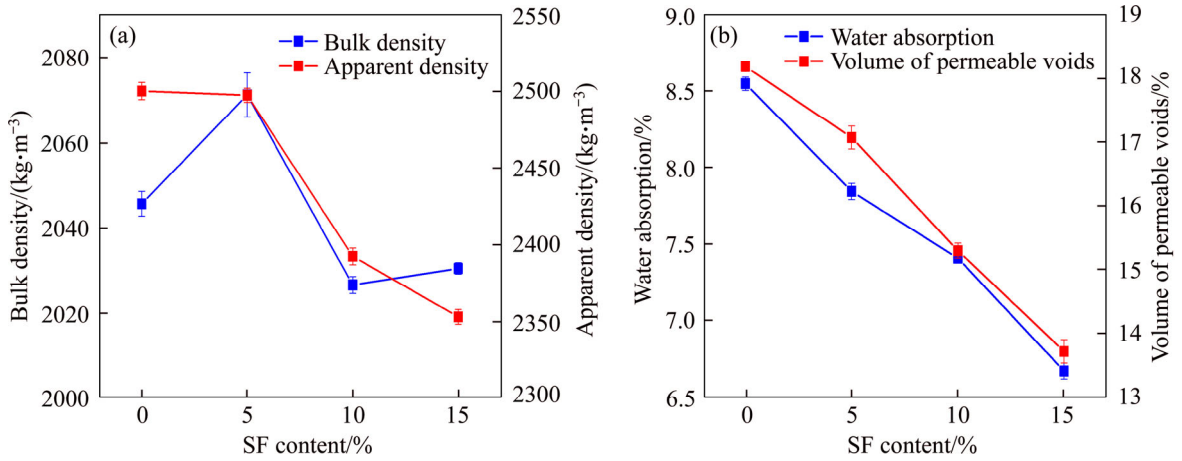

Figure 2 Density, water absorption and volume of permeable voids of SF mixtures: (a) Bulk density and apparent density; (b) Water absorption and volume of permeable voids

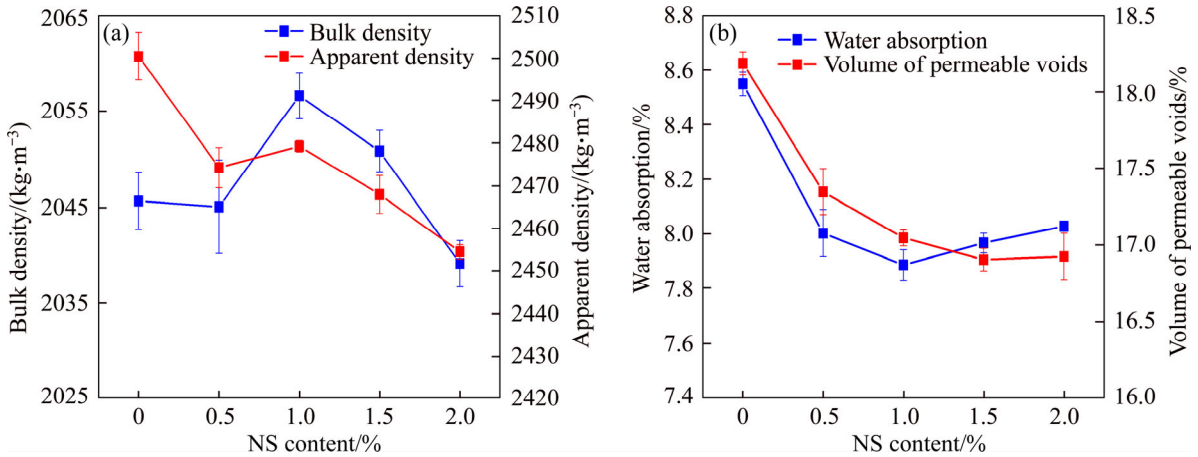

Figure 3 Density, water absorption and volume of permeable voids of NS mixtures: (a) Bulk density and apparent density; (b) Water absorption and volume of permeable voids

content, reaching 2030.5 kg/m^3 for the mixture with 15% silica fume. The increased bulk density at 5% silica fume could have been due to the reduced porosity that resulted from the generation of secondary C-S-H from pozzolanic reaction [45] and from the pore-filling effects of silica particles [46]. The reduced bulk density at higher silica fume content could have been caused by the lower specific gravity of silica fume (2.2−2.3 compared with 3.15 for Portland cement). The increase in silica fume dosage reduces the availability of CH for pozzolanic reaction, thus leads to a higher content of unreacted silica fume. The unreacted particles acted as either inert filler or defects in the matrix [47] that reduced the bulk density of samples. The existence of unreacted silica fume can be confirmed from the TGA results in this study by comparing the actual and theoretical CH content which can be calculated based on the method proposed by RUPASINGHE et al [48] and DODSON et al [49], respectively. It was found that the actual CH content was around 23%, 20% and 18% for the mixture with 5%, 10% and 15% of silica fume, respectively, while the corresponding theoretical values were around 20%, 16% and 13%. Higher actual CH contents than the theoretical values suggest that only part of the silica fume was reacted. Another contributing reason for the reduced bulk density is the generated low Ca/Si CSH. The CSH generated from the pozzolanic reaction has a lower Ca/Si ratio than that of CSH from the cement hydration [50, 51]. It was found that the density of CSH is linearly proportional to the Ca/Si ratio. A lower Ca/Si ratio leads to a lower density of CSH [52, 53]. The apparent density generally decreased with the increase of silica fume content. It reduced from 2500.4 kg/m^3 for the reference mixture to 2353 kg/m^3 for the mixture with 15% silica fume. The reduction in apparent density suggests that the volume of impermeable voids is increased [40]. It was found that the silica fume addition led to an increase in pores smaller than 40 nm for mortar samples [54], which are more impermeable [55]. The increased C-S-H gel from the pozzolanic reaction may be responsible for the increase in the impermeable voids, as gel pores <20 nm coexist with C-S-H gel [56, 57]. Figure 2(b) illustrates the results of water absorption and the volume of permeable voids for mixtures with silica fume. Both the water absorption and volume of permeable voids were decreasing with the increase of silica fume content. Water absorption decreased from 8.55% for the reference mixture to 6.67% for the mixture with 15% silica fume, while the volume of permeable voids reduced from 18.19% to 13.71%. This finding is in good agreement with previous research. WU et al [17] found that the volume of permeable voids was decreasing with silica fume content until it reached 20%. The reduced water absorption and volume of permeable voids suggests a reduction in large pores. This finding coincides with previous studies. TORII et al [54] found through a mercury intrusion test that the silica fume addition reduced the pores larger than 100 nm, which are water-permeable pores. Similarly, YAJUUN et al [58] observed that the pores larger than 10 nm decreased significantly from 19.38% for the reference mixture to 15.06% for the mixture with 15% silica fume.

Figure 3(a) shows the results of bulk density and the apparent density of mixtures containing nano-silica. The bulk density generally increased with nano-silica content from 2045.7 kg/m^3 for the reference mixture to 2056.6 kg/m^3 for the mixture with 1% nano-silica. This can be attributed to the pore-filling effect [46] and the enhanced cement hydration that made the mortar denser (see Section 3.1.2). Then, the bulk density was reduced when more cement was replaced with nano-silica, reaching 2039.1 kg/m^3 for the mixture with 2% nano-silica. The particle agglomeration could be responsible for this reduction. It was found that ≥1.5% nano-silica led to significant agglomeration, which acted as defects in mortar samples [37]. The agglomerated particles acted as defects in mortar samples that reduced the bulk density. The apparent density, however, was reduced with the increase of nano-silica content. The mixture with higher nano-silica content showed lower apparent density. The reference mixture had an apparent density of 2500.4 kg/m^3, and the apparent density was reduced to 2454.6 kg/m^3 for the mixture with 2% nano-silica. The decrease in apparent density suggests that the volume of impermeable voids was increased with the nano-silica addition. This is in good agreement with the research of others. LI et al [59] found that the addition of nano-silica up to 4% increased pores smaller than 20 nm, while WU et al [60] observed an increase in pores smaller than 50 nm with nano-silica content up to 2.0%.

Figure 3(b) illustrates the water absorption and volume of permeable voids for nano-silica mixtures. The water absorption decreased slightly from 8.55% for the reference mixture to 7.89% for the mixture with 1.0% nano-silica. The further addition of nano-silica increased the water absorption to 8.03% for the mixture with 2.0% nano-silica. This coincides with the findings by WU et al [60], which revealed that the mixture with 1% nano-silica showed the lowest porosity. A similar trend was observed for the volume of permeable voids, except the lowest value was found at 1.5% nano-silica content. The increase in water absorption at a dosage >1% could be due to the particle agglomeration that acts as defects in the mortar sample [37].

Compared with nano-silica, silica fume showed a more significant influence on density and microstructure. For example, the water absorption was reduced from 8.55% to 6.67% by a 15% silica fume addition, while the lowest water absorption was 7.89% at a 1% nano-silica addition. Similar findings on the microstructure of mixtures with silica fume and nano-silica were reported in previous research. JALAL et al [61] found the capillary water absorption and chloride ion penetration of a mixture with 10% silica fume were lower than that with 2% nano-silica. A possible reason for this is that the extremely fine particle size of nano-silica can only affect a narrow range of pores. KONG et al [62] found that silica fume with a large particle size was more effective in reducing macropores, while nano-silica was found to be more efficient in refining micropores. FOROOD et al [63] found a nano-silica addition to mixtures with a water-to-binder ratio of 0.65 significantly reduced porosity for pores between 20−50 nm, but only a marginal reduction in porosity was found for pores larger than 50 nm.

3.1.2 Thermo-gravimetric analysis

A thermo-gravimetric analysis (TGA) was conducted to evaluate the influence of silica fume and nano-silica on the hydration of cement-based composites. The results are shown in Figure 4. There are three main phases of weight loss. The first phase of weight loss starts from room temperature (~20 °C) to 400 °C, which results from the dehydration of C-S-H gel and ettringite [64]. The second phase of weight loss ends at around 560 °C [48]. The dehydration of CH is responsible

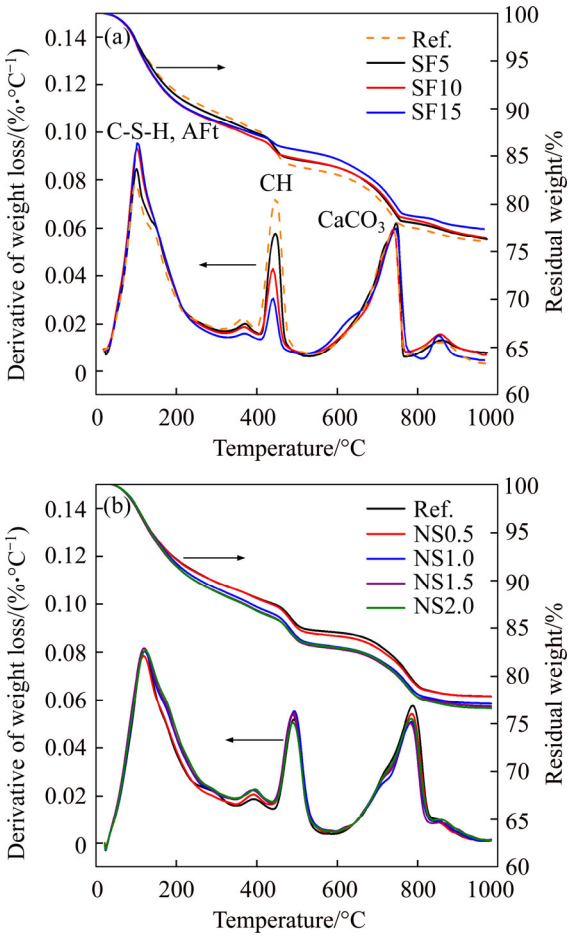

Figure 4 TG/DTG curves of mortar mixtures: (a) Silica fume; (b) Nano-silica

for the weight loss at this phase. The last phase of weight loss, starting from 560 °C to 840 °C is caused by the decarbonization of $CaCO_3$ [48].

Figure 4(a) shows the thermo-gravimetric (TG) and derivative of thermo-gravimetric (DTG) curves of mixtures with silica fume. It is noticed that the peak of CH on the DTG curves reduced with the increase of silica fume content, while the peak of C-S-H was increased with the silica fume content. This is attributed to the pozzolanic reaction between CH and silica fume, which consumes CH and generates secondary C-S-H gel [65]. With the increase in silica fume content, more CH is consumed, generating more C-S-H gel, which caused the reduction of the CH peak and the increase of the C-S-H peak on the DTG curves.

Compared with the mixtures with silica fume, the addition of nano-silica showed less pozzolanic reaction as a negligible reduction of CH peak was observed for mixtures with nano-silica. This may be caused by the lower dosage of nano-silica than that

of silica fume. Despite the low pozzolanic reaction, the substitution of cement with nano-silica increased the final weight loss. The reference mixture had a final weight loss of 22.15%, while a weight loss of 22.17%, 22.95%, 23.22% and 23.44% was found for mixtures with 0.5%, 1.0%, 1.5% and 2.0% of nano-silica, respectively. The increase in the final weight loss could be caused by the improved hydration caused by the nucleation effect [66] and the generation of secondary C-S-H from the pozzolanic reaction. It can be seen from the TG curves that the mixtures with nano-silica showed less residual weight at a temperature of 400 °C than that of the reference mixture, which suggests that there was more C-S-H gel in the mixtures with nano-silica.

3.1.3 Mechanical strength

Mechanical strength is critical for underground structure performance as it indicates the bearing capacity of the structure. In this study, the UCS was tested after 28 d of standard curing. The results are plotted in Figure 5. The addition of nano-silica and silica fume enhanced the UCS of mortar samples. The UCS increased from 34.429 MPa for the reference mixture to 40.159 MPa for the mixture with 1.0% of nano-silica, which accounts for a 16.64% improvement. Then, it dropped back to 35.524 MPa at 2.0% nano-silica. Improved compressive strength has also been reported in previous research [23, 67, 68]. For example, an improvement of 9% and 12% in UCS was observed by DU et al [67] for concrete mixtures with 0.3% and 0.9% nano-silica, respectively. The enhanced UCS may be attributed to the reduced porosity, which is confirmed by the results of water absorption and the volume of permeable voids. Compared with the nano-silica mixtures, silica fume incorporation showed more significant enhancement of UCS. The UCS increased to 52.7 MPa at 10% silica fume, accounting for a 47% improvement. Then, the UCS reduced to 48.9 MPa at 15% silica fume. This finding coincides with results in previous research. AL-SWAIDANI et al [69] found that a mixture with a nano-silica content of less than 3% showed lower compressive strength than a mixture with 10% silica fume. This more drastic improvement in UCS by silica fume could be due to the lower volume of water-permeable voids and more significant pozzolanic reaction. It was observed that the silica fume is more effective

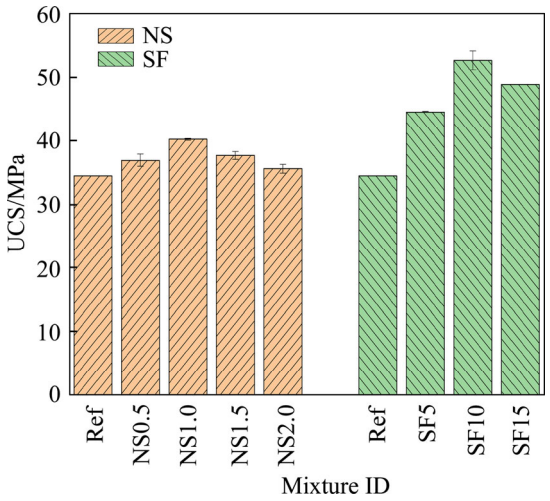

Figure 5 UCS of mixtures after 28 d of curing

at reducing the porosity of mortars, as discussed in Section 3.1.1. In addition, the TGA results illustrated that the pozzolanic reaction in mixtures with silica fume was more significant than that in mixtures with nano-silica.

3.2 Properties after sulfuric acid immersion

3.2.1 Visual observation

Visual observation was conducted as one of the evaluation methods of sample deterioration. Figure 6 shows the cross-section of samples after phenolphthalein spray. The purple area indicates the unneutralized area, while the white/grey area is the neutralized area. From Figure 6, the reference sample was severely corroded because a ~1.5 mm thick neutralized layer was clearly observed at the surface of the reference sample. With the substitution of 5% silica fume, the thickness of the neutralized layer was significantly reduced. As shown in Figure 6(b), the neutralized layer is noticeably thinner. By adding more silica fume, the neutralized layer became thicker. A neutralized layer of about 2 mm thick was observed for mixtures with 10% and 15% of silica fume. It is also noted that a lower volume of permeable voids did not necessarily lead to a thinner neutralized layer. This is because the addition of silica fume affects a group of mortar properties that influences the acid resistance, including porosity, neutralization capability, and chemical stability. First, the addition of silica fume reduced the volume of permeable voids due to the pozzolanic reaction [45] and pore-filling effect [46]. The reduced volume of permeable voids hindered the

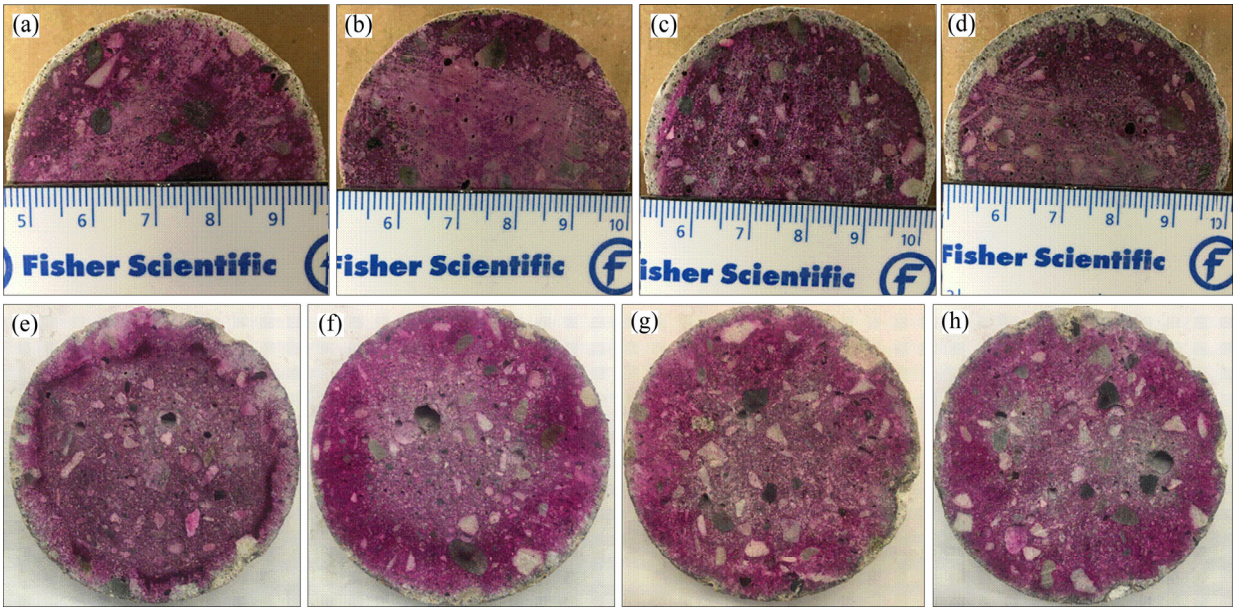

Figure 6 Visual observation: (a) Reference; (b) SF5; (c) SF10; (d) SF15; (e) NS0.5; (f) NS1.0; (g) NS1.5; (h) NS2.0

acid penetration, thus reduced the corrosion degree. Second, the chemical stability of samples was increased due to the consumption of CH and the generation of CSH from the pozzolanic reaction. It is reported that the CSH from the pozzolanic reaction has a low Ca/Si ratio, which leads to a more stable structure [50, 51]. Third, the replacement of cement by silica fume reduced the content of cement hydration products, thus reduced the neutralization capability. It has been reported that higher neutralization capability could lead to a higher acid resistance [70, 71]. This reduced neutralization capability led to a thick neutralized layer of about 2 mm at 10% and 15% of silica fume.

For mixtures with nano-silica, inhibited corrosion can be observed compared with the reference mixture as the corrosion layers are relatively thin. But it is difficult to tell which sample showed better performance as the boundary between the neutralized area and the unneutralized area is not clear. Thus, more indicators (e.g., mass change and length change) should be used to evaluate the acid resistance.

3.2.2 Mechanical strength

The UCS and UCS change after 75 d of acid immersion are illustrated in Figure 7. The positive UCS change means a UCS increase, while the negative UCS change indicates a UCS loss. For mixtures with nano-silica, all mixtures showed a positive UCS change. The reference mixture had a

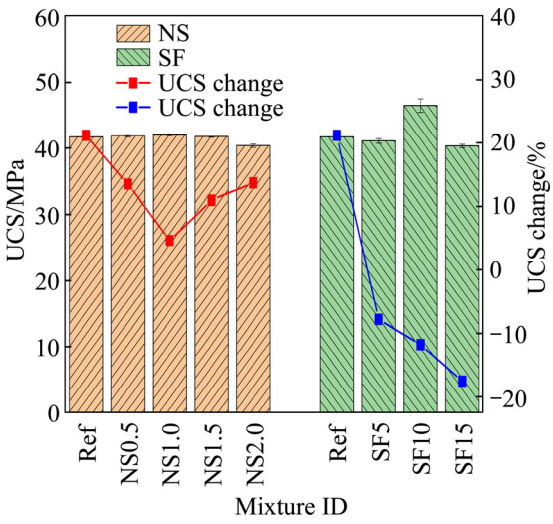

Figure 7 UCS and UCS change after 75 d of sulfuric acid immersion

UCS change of 21%. The UCS change dropped with the increase of nano-silica content, reaching 4.6% at 1% nano-silica. Then, the UCS change increased again to 13.69% at 2% nano-silica. After the 75 d of sulfuric acid immersion, all mixtures showed a similar UCS of ~42 MPa. A UCS increase during sulfuric acid immersion was also reported in previous research. For example, MAKHLOUFI et al [72] investigated the compressive development of mortars with blended cement during sulfuric acid immersion. It was found that all Portland cement mixtures demonstrated a compressive strength increase during immersion, with the highest strength increase of 30% at the immersion age of

180 d. They attributed the increase in compressive strength to the continuous hydration of cement. Similarly, RAHMANI et al [73] investigated the strength development of Portland-cement-based concrete mixtures under sulfuric acid attack. A strength increase of up to 11.2% was observed after 28 d of sulfuric acid immersion. They attributed the strength increase to the continuous hydration and the filler effect of generated gypsum and ettringite. The continuous hydration has been confirmed in previous research. For example, FENG et al [74] found that the CH content in Portland cement paste increased from 18.36% after 28 d of curing to 21.2% after 90 d of curing. In addition, AL-SWAIDANI et al [75] observed a UCS increase of 10−15 MPa from 28 d to 90 d of standard curing. In terms of the filler effect of corrosion product, TSUBONE [76] found that the total pore volume near the boundary between the corroded part and the uncorroded part was smaller than that in the inner uncorroded part. This suggests that the pores may be filled by the gypsum produced.

Contrary to mixtures with nano-silica, all mixtures with silica fume showed negative UCS change. The mixture with a higher content of silica fume showed a higher UCS loss. The reference mixture had a UCS change of 21%, while the mixture with 15% silica fume showed a UCS change of −17.5%. After 75 d of sulfuric acid immersion, the mixture with 10% silica fume showed the highest UCS with a value of 46.47 MPa. The other three mixtures showed a similar UCS of 42 MPa. The negative UCS change of silica fume mixtures may be caused by the enhanced hydration before sulfuric acid immersion. HUANG et al [77] observed that the silica fume particles acted as nucleation sites during cement hydration, which accelerates the cement hydration reaction. More specifically, KADRI et al [78] observed a higher heat release rate of silica fume mixtures at earlier stages compared with that of the reference mixture. This accelerated hydration mitigated the effect of continuous hydration on strength development during sulfuric acid immersion.

3.2.3 Ultrasonic pulse velocity

The test of UPV is increasingly adopted as a non-destructive method to assess the deterioration of cement-based composites [7, 22, 79, 80]. In this research, the UPV was monitored during sulfuric acid immersion as a possible indicator of sample deterioration. A high UPV indicates a dense microstructure and fewer cracks [7]. Figure 8 presents the UPV results of mixtures with silica fume and mixtures with nano-silica. Before sulfuric acid immersion, the UPV of mixtures with nano-silica ranged from 4070−4193 m/s, which can be classified as being of good quality (3600−4500 m/s) [81, 82]. The addition of nano-silica and silica fume enhanced the UPV of mortar samples. For example, the addition of nano-silica increased the UPV from 4070 m/s for the reference mixture to 4193 m/s for the mixture with 0.5% nano-silica. This can be attributed to the reduced porosity, which has been confirmed in Section 3.1.1. Compared with the nano-silica mixtures, the silica fume addition showed a more significant enhancement in the UPV. The mixture with a 5% silica fume showed the highest UPV of 4343.3 m/s.

During sulfuric acid immersion, the UPV of all mixtures was decreasing with the immersion time. This was caused by the formation of a corrosion layer on the sample surface (see Section 3.2.1), which has a porous structure. As shown in

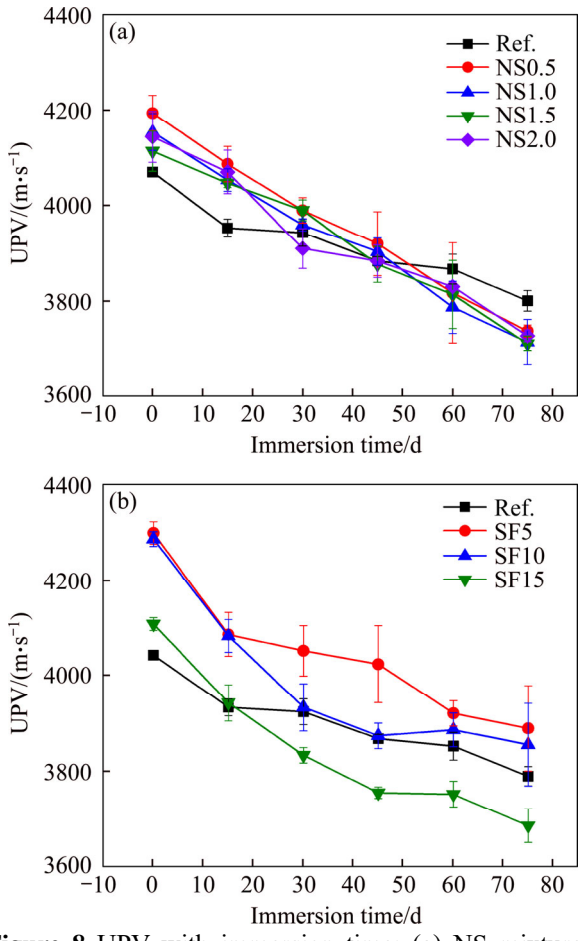

Figure 8 UPV with immersion time: (a) NS mixtures; (b) SF mixtures

Figure 8(a), the addition of nano-silica showed a limited effect on the UPV throughout the immersion period as mixtures with nano-silica showed similar UPV values at all ages. After 75 d of immersion, the UPV of mixtures with nano-silica ranged from 3710 to 3800 m/s, which indicates that the samples were still of good quality. However, the mixtures with nano-silica had a lower UPV than the reference mixture. Compared with mixtures with nano-silica, the mixtures with silica fume showed a higher UPV. It ranged from 3690 to 3906 m/s after sulfuric acid immersion. The highest UPV was found on the mixture with 5% of silica fume.

3.2.4 Length change

The sulfuric acid corrosion may result in a length change due to the dissolution of cement hydrates and the peeling off of aggregates. Thus, the change in length was monitored as one of the indicators to evaluate sample deterioration. The length change of mixtures with nano-silica is demonstrated in Figure 9. A positive value implies that the sample length was increased. As shown in Figure 9(a), all samples showed a positive length change throughout the immersion period, and the length change increased with immersion time. The reference mixture had the lowest length increase throughout the immersion period. It is also noticed that the nano-silica dosage showed a negligible effect on the length change since the length change of mixtures with nano-silica was similar at all immersion ages. The length change after 75 d of immersion is plotted in Figure 9(b). Before sample brushing, the reference mixture had a length change of 0.12%. The greatest length change of 0.47% was found for the mixture with 2% nano-silica. This positive length change was caused by the generation of gypsum, which is two times larger than cement hydration products [83]. The length of the samples was also measured after removing the corrosion layer on sample surface, and the results are shown in Figure 9(b) with a blue line. All samples showed a negative length change after removing the corrosion layer. The reference mixture showed a length change of −1.34%. The nano-silica addition slightly reduced the length change to −0.93% for the mixture with 1 % nano-silica. With nano-silica content higher than 1%, a greater length change was observed, with a value of −1.22% for the mixture with 2% nano-silica. The higher length loss at nano-silica >1% could be due to the

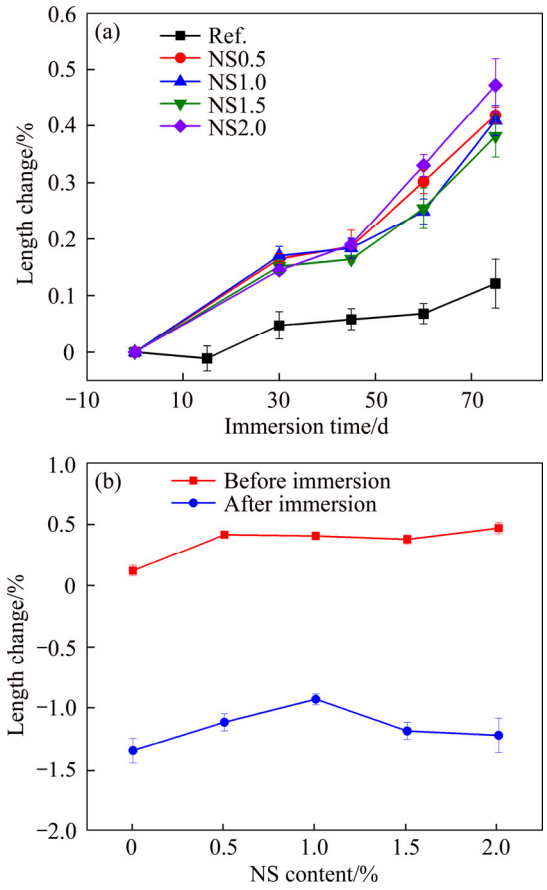

Figure 9 Length change of NS mixtures: (a) With immersion time; (b) With NS content after sulfuric acid immersion

increased water absorption caused by the agglomeration of nano-silica, which has been confirmed in Section 3.1.1. The increased water absorption enhanced acid penetration and led to a higher length loss.

The length change of silica fume mixtures is presented in Figure 10. Similarly, the mixtures with silica fume also showed a positive length change during immersion. The length change also increased with immersion time. The reference mixture had the lowest length change, while the mixture with 5% silica fume showed the greatest length change in the entire immersion period. The length change after 75 d of sulfuric acid immersion is plotted in Figure 10(b). The mixture with a 5% silica fume showed the greatest length change of 0.43%. After sample brushing, the corrosion layer on the sample surface was removed. The length change after sample brushing is plotted in Figure 10(b) with a blue line. All mixtures showed a negative length change. The lowest length change of −0.57% was observed on the mixture with 5% silica fume. This

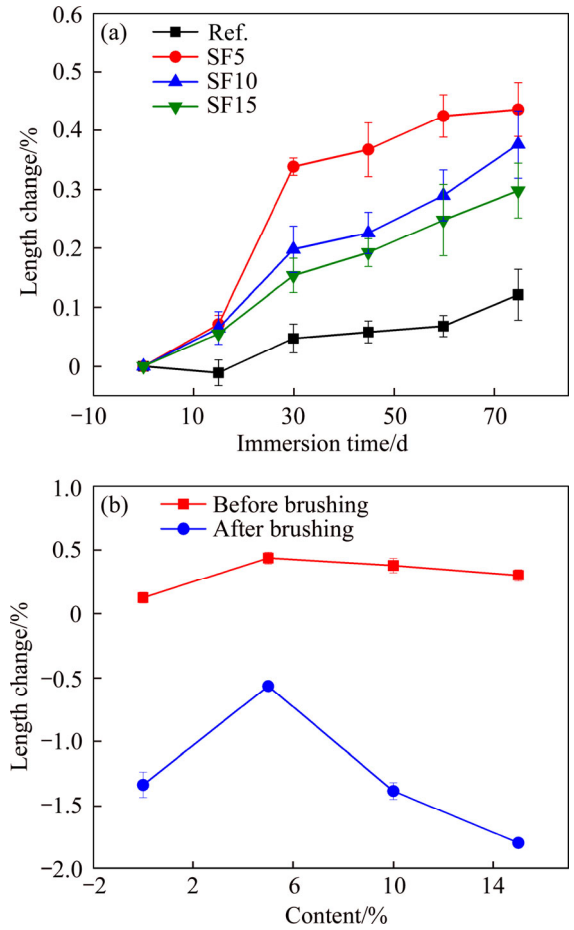

Figure 10 Length change of SF mixtures: (a) With immersion time; (b) With SF content after sulfuric acid immersion

may suggest that the mixture with 5% silica fume has the highest acid resistance. The reduced volume of permeable voids and the increased chemical stability were responsible (as discussed in Section 3.2.1) for the reduced length change for the mixture with 5% of silica fume.

3.2.5 Mass change

Sulfuric acid corrosion can lead to a loss of sample due to the dissolution of cement hydrates and the peeling off of aggregates. Thus, the change in mass was monitored as another parameter to assess sample deterioration during sulfuric acid immersion. Figure 11 illustrates the mass change of mixtures with nano-silica. A positive value indicates mass gain, while a negative value indicates a mass loss. In general, the mass change of all mixtures increased with immersion time for all mixtures. After 75 d of immersion, the mixtures had a mass change ranging from 0.835% to 1.383%, with the mixture with 0.5% nano-silica having the lowest mass change. The increased mass during acid immersion was due to the generation of gypsum that attached to the sample surface (as shown in the visual observation results). To better understand the sample deterioration, the corrosion layer was removed by brushing the samples with a steel brush. The mass change after sample brushing is shown in Figure 11(b). All mixtures showed a negative mass change after brushing. The mass loss reduced from −5.48% for the reference mixture to −4.06% for the mixture with 1% nano-silica, and then the mass loss increased to −4.9% for the mixture with 2% nano-silica. This suggests that the addition of 1% of nano-silica mitigated the deterioration in terms of mass change.

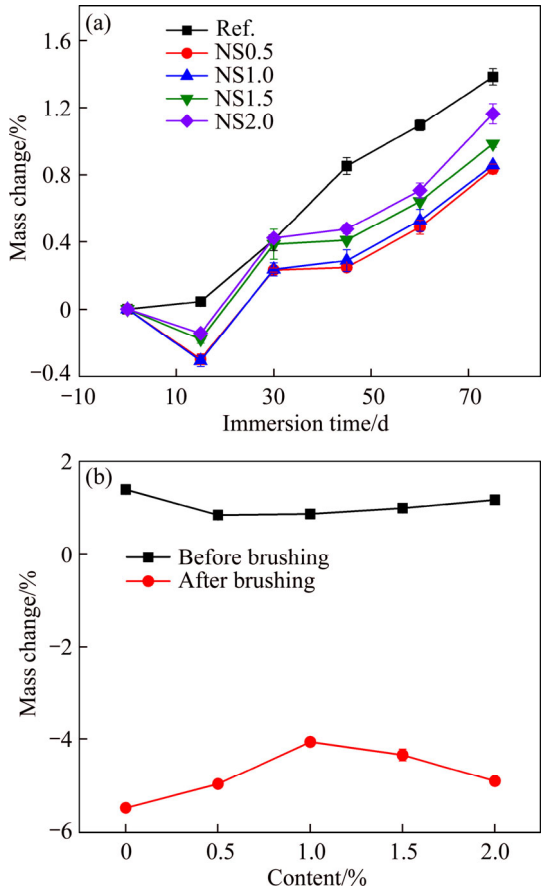

Figure 11 Mass change of NS mixtures: (a) With immersion time; (b) With NS content after sulfuric acid immersion

The mass change of silica fume mixtures is plotted in Figure 12. Similarly, all mixtures illustrated positive mass change during the immersion period. The mass change after 75 d of immersion ranged from 1.12% for the mixture with 15% silica fume to 1.56% for the mixture with 5% silica fume. After the corrosion layer was removed by brushing, all samples illustrated mass loss.

Among the mixtures, the one with 5% silica fume showed the lowest mass loss with a value of −4.15%, compared with −5.48% for the reference mixture. Adding more than 5% silica fume increased the mass loss to −6.63% for the mixture with 15% silica fume. This suggests that the mixture with 5% silica fume showed the best acid resistance in terms of mass change. Compared with nano-silica mixtures, the silica fume mixtures generally showed a higher mass change. The mass change of nano-silica mixtures ranged from −5.48% to −4.06%, while the mass change of silica fume mixtures ranged from −6.63% to −4.15%. This can be attributed to the differences in neutralization ability between these mixtures. As observed in the TGA results, the addition of 15% silica fume reduced the final weight loss (1.35%), while the addition of 2% of nano-silica increased the final weight loss (1.29%). This suggests that the mixtures with nano-silica had a higher content of cement hydration products, which led to a higher neutralization.

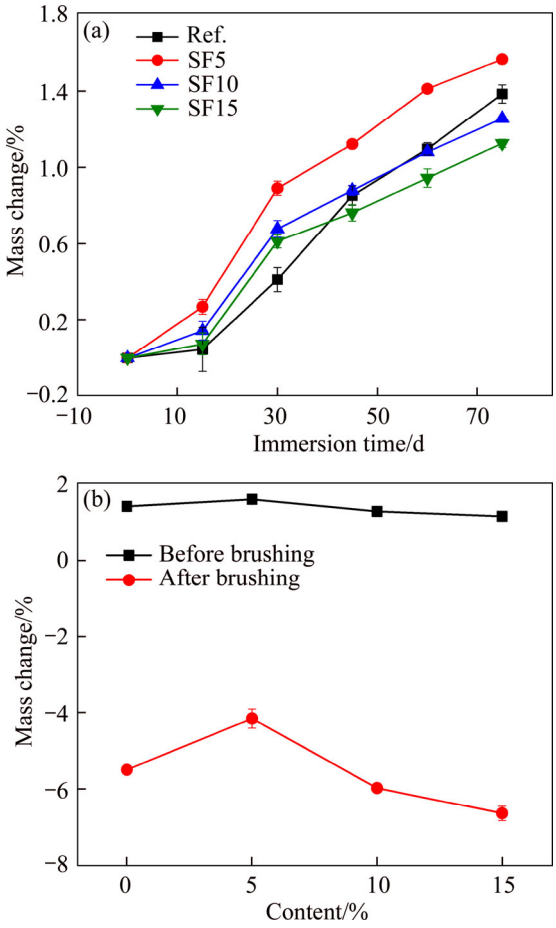

Figure 12 Mass change of SF mixtures: (a) With immersion time; (b) With SF content after sulfuric acid immersion

3.3 Evaluation of acid resistance

During the sulfuric acid immersion, several tests were conducted to evaluate the acid resistance of mixtures with nano-silica and silica fume. Due to the generation of a corrosion layer on the samples' surface, both mass and length increased during sulfuric acid immersion. And the mass change and length change had a good correlation with R^2 of 0.86 and 0.83 for mixtures with nano-silica and silica fume, respectively, as shown in Figure 13. However, the positive mass change and length change made the evaluation of sample deterioration difficult because of the complexity of the mechanism of the mass change and length change during immersion. On the one hand, when samples are immersed in sulfuric acid, the CH and C-S-H are decalcified at the presence of H^+ in the pore solution [84]. This reduces the mass and length of samples. On the other hand, the chemical reaction between cement hydration products (e.g., CH and C-S-H) and the sulfuric acid generates swelling gypsum that will lead to the formation of a corrosion layer on the sample surface. This causes

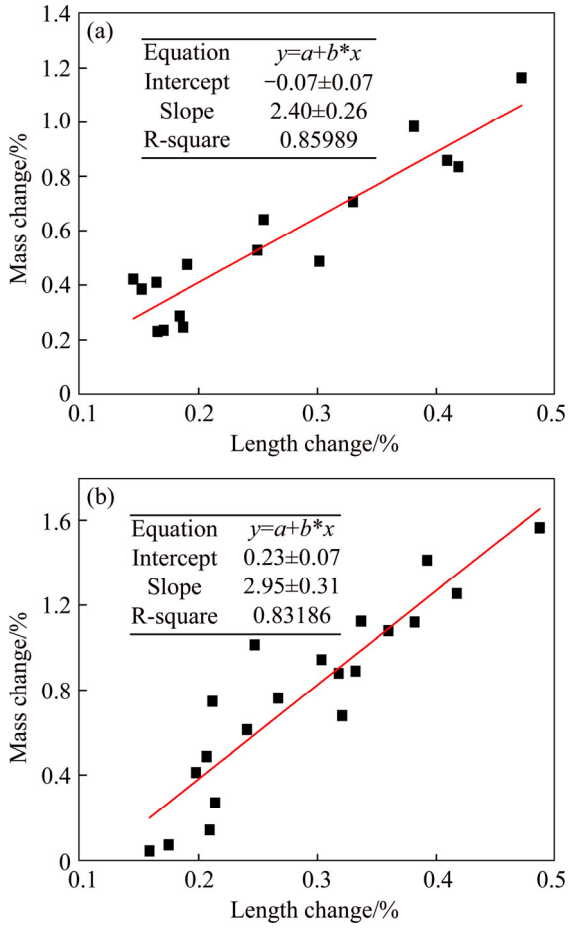

Figure 13 Correlation between length change and mass change (before brush): (a) NS mixtures; (b) SF mixtures

the mass and length increase during immersion. Thus, to remove the effect of gypsum generation on the mass change and length change, sample brushing with a steel brusher was carried out on samples after 75 d of immersion. The results after brushing showed that the mixture with 5% silica fume and 1% nano-silica had the lowest mass change and length change for silica fume mixtures and nano-silica mixtures, respectively. This reduced deterioration on samples can be attributed to the reduced volume of permeable voids, enhanced chemical stability and cement hydration, as discussed in Sections 3.1.1 and 3.1.2. Beyond these dosages, higher mass loss and length loss were observed. For mixtures with nano-silica, a possible reason for this is the nano-silica agglomeration that became weak zones in the mortar sample; for mixtures with silica fume, the reduced neutralization capacity was responsible for the high deterioration at high dosage.

However, the UCS and UPV results suggest that other mixtures may have a better performance after sulfuric acid immersion. For example, the reference mixture showed a positive UCS change, while all the silica fume mixtures showed reduced UCS after sulfuric acid exposure. In addition, the UPV results indicated that the mixture with nano-silica was of lower quality compared with the reference mixture after 75 d of sulfuric acid immersion. These contradictory results from various indicators may suggest that there is no single indicator that is able to comprehensively describe the deterioration [85]. GU et al [85] compared test methodologies regarding the assessment of deterioration. They concluded that each test method has the following disadvantages: 1) visual observation is a subjective judgment and can be significantly influenced by samples palling; 2) mass change is highly variable because of the peeling off of the aggregates; 3) the length is too sensitive to pH change, and may have a high error on rough surfaces. The change in UCS, however, was found in this research to be highly affected by the hydration degree of samples before immersion. At a low hydration degree, such as for the reference mixture, the UCS could be increased during sulfuric acid immersion due to the continuous hydration. This makes the UCS change a poor indicator of sample deterioration. One indicator can only partially reflect the deterioration samples. A combination of indicators should be used to comprehensively assess the acid resistance of mixtures.

Among all the silica fume mixtures, the one with 5% silica fume showed the best performance in resisting sulfuric acid attack because it had the lowest mass change and length change. In addition, the mixture showed a reasonably high UCS and UPV after sulfuric acid immersion. Similarly, for mixtures with nano-silica, the mixture with 1% nano-silica presented the lowest mass change and length change and a reasonably high UCS. This suggests that for the mixtures with nano-silica, a 1% addition has the best potential with regard to resisting sulfuric acid. It is also noted that the silica fume was noticeably more effective than nano-silica in enhancing the acid resistance of mortars as the mixture with 5% silica fume showed less length change, and higher UCS and UPV than the mixture with 1% nano-silica after 75 d of immersion.

4 Conclusions

The mortar samples with silica fume and nano-silica were immersed in sulfuric acid (pH=2) for 75 d to investigate acid resistance. From the test results, the following conclusions can be drawn:

1) From the density, water absorption, and permeable voids results, the addition of silica fume and nano-silica reduced the water absorption and volume of permeable voids. In addition, the silica fume showed a more drastic influence on the water absorption and volume of permeable voids compared with nano-silica.

2) From the thermo-gravimetric analysis result, the addition of silica fume significantly reduced calcium hydroxide and increased calcium silicate hydrates in the hardened samples. This is attributed to the pozzolanic reaction between calcium hydroxide and silica fume. The addition of nano-silica showed a negligible effect on cement hydration as there was no significant change in the amount of calcium hydroxide and calcium silicate hydrates.

3) The addition of nano-silica and nano-silica improved the unconfined compressive strength after 28 d of curing. However, the silica fume showed more significant improvement than that of nano-silica, with the greatest improvement of 16.7% and 47% for nano-silica mixtures and silica fume

mixtures, respectively.

4) The sulfuric acid immersion test illustrated that the silica fume was more effective than nano-silica in improving the acid resistance of cement mortars. The optimal dosages with best acid resistance were 1% and 5% for nano-silica and silica fume, respectively. However, the mixture with 5% silica fume illustrated noticeably better performance than the one with 1% nano-silica as it had less length change, and higher compressive strength and ultrasonic pulse velocity after 75 d of immersion.

5) The selection of indicators for deterioration evaluation could significantly affect the evaluation of acid resistance because contradictory results were found from different test methods. This suggests that there is no single indicator that is able to describe the deterioration comprehensively.

Acknowledgment

The authors are thankful for the financial support by the Natural Sciences and Engineering Research Council of Canada (NSERC RGPIN-2017-05537) and the generous donation of Aerosol-fumed silica from Evonik Industries.

Contributors

WU Lin-ping was responsible for experimental design, data collection and analysis, and manuscript writing. LIU Wei Victor was involved in concept formation and contributed to manuscript composition and edits. HUANG Guang-ping helped in data collection and manuscript edits.

Conflict of interest

The authors declare that they have no conflict of interest.

References

[1] DORION J F, HADJIGEORGIOU J. Microbiologically influenced corrosion (MIC) of ground support [J]. Geotechnical and Geological Engineering, 2020, 38(1): 375−387. DOI: 10.1007/s10706-019-01028-3.

[2] WU L, HU C, LIU V W. The sustainability of concrete in sewer tunnel—A narrative review of acid corrosion in the city of Edmonton, Canada [J]. Sustainability, 2018, 10(2). DOI: 10.3390/su10020517.

[3] CARATELLI A, MEDA A, RINALDI Z, ROMUALDI P, Structural behaviour of precast tunnel segments in fiber reinforced concrete [J]. Tunnelling and Underground Space Technology, 2011, 26(2): 284−291. DOI: https://doi.org/10.1016/j.tust.2010.10.003.

[4] YU H, WU L, LIU W, POURRAHIMIAN Y. Effects of fibers on expansive shotcrete mixtures consisting of calcium sulfoaluminate cement, ordinary Portland cement, and calcium sulfate [J]. Journal of Rock Mechanics and Geotechnical Engineering, 2018, 10(2): 212−221. DOI: https://doi.org/10.1016/j.jrmge.2017.12.001.

[5] ERGÜLER G K. Investigation the applicability of eggshell for the treatment of a contaminated mining site [J]. Minerals Engineering, 2015, 76: 10−19. DOI: https://doi.org/10.1016/j.mineng.2015.02.002.

[6] JONES S N, CETIN B. Remediation of acid mine drainages with recycled concrete aggregates [J]. Geotechnical Frontiers, 2017. DOI: https://doi.org/10.1061/9780784480434.049.

[7] JEON I K, QUDOOS A, JAKHRANI S H, KIM H G, RYOU J S. Investigation of sulfuric acid attack upon cement mortars containing silicon carbide powder [J]. Powder Technology, 2020, 359: 181−189. DOI: https://doi.org/10.1016/j.powtec.2019.10.026.

[8] LI J, ZHANG T, LIU T. Corrosion of cement-based support system by acidic water in a deep copper mine [J]. Mordern Mining, 2018(591): 226−229. (in Chinese)

[9] KAUFMANN J. Durability performance of fiber reinforced shotcrete in aggressive environment [C]// World Tunnelling Congress. Foz do Iguaçu, Brazil. 2014: 1−7.

[10] EKOLU S O, DIOP S, AZENE F, MKHIZE N. Disintegration of concrete construction induced by acid mine drainage attack [J]. Journal of the South African Institution of Civil Engineers, 2016, 58(1): 34−42. DOI: 10.17159/2309-8775/2016/v58n1a4.

[11] ERCIKDI B, KESIMAL A, CIHANGIR F, DEVECI H, ALP İ. Cemented paste backfill of sulphide-rich tailings: Importance of binder type and dosage [J]. Cement and Concrete Composites, 2009. 31(4): 268−274. DOI: https://doi.org/10.1016/j.cemconcomp.2009.01.008.

[12] YIN S, SHAO Y, WU A, RAO Y, CHEN X. Deformation behaviors of cemented backfill using sulphide-content tailings [C]// Proceedings of the 20th International Seminar on Paste and Thickened Tailings. Beijing: University of Science and Technology Beijing, 2017: 315−327. DOI: 10.36487/ACG_REP/1752_35_YIN.

[13] TARIQ A, YANFUL E K. A review of binders used in cemented paste tailings for underground and surface disposal practices [J]. Journal of Environmental Management, 2013, 131: 138−149. DOI: https://doi.org/10.1016/j.jenvman.2013.09.039.

[14] HAGELIA P. Durability development in sprayed concrete for rock support; Is it possible to establish a basis for modelling? [J]. Heron, 2019, 64(1/2): 75−96.

[15] TORII K, KAWAMURA M. Effects of fly ash and silica fume on the resistance of mortar to sulfuric acid and sulfate attack [J]. Cement and Concrete Research, 1994, 24(2): 361−370. DOI: http://dx.doi.org/10.1016/0008-8846(94)90063-9.

[16] MEHTA P. Studies on chemical resistance of low water/cement ratio concretes [J]. Cement and Concrete Research, 1985, 15(6): 969−978. DOI: https://doi.org/10.1016/0008-8846(85)90087-0.

[17] WU L, HU C, LIU W V. Effects of pozzolans on acid resistance of shotcrete for sewer tunnel rehabilitation [J]. Journal of Sustainable Cement-Based Materials, 2019, 8(1): 55−77. DOI: 10.1080/21650373.2018.1519645.

[18] MEHTA P K. Properties of blended cements made from rice husk ash [J]. Journal of the American Concrete Institute, 1977, 74(9): 440−442. DOI: 10.14359/11022.

[19] GUTBERLET T, HILBIG H, BEDDOE R. Acid attack on hydrated cement—Effect of mineral acids on the degradation process [J]. Cement and Concrete Research, 2015, 74: 35−43. DOI: https://doi.org/10.1016/j.cemconres.2015.03.011.

[20] AMIN M, BASSUONI M T. Response of concrete with blended binders and nanoparticles to sulfuric acid attack [J]. Magazine of Concrete Research, 2017, 70(12): 617−632. DOI: https://doi.org/10.1680/jmacr.17.00081.

[21] DUAN P, SHUI Z, CHEN W, SHEN C. Effects of metakaolin, silica fume and slag on pore structure, interfacial transition zone and compressive strength of concrete [J]. Construction and Building Materials, 2013, 44: 1−6. DOI: http://dx.doi.org/10.1016/j.conbuildmat.2013.02.075.

[22] DIAB A M, ELYAMANY H E, ELMOATY A E M A, SREH M M. Effect of nanomaterials additives on performance of concrete resistance against magnesium sulfate and acids [J]. Construction and Building Materials, 2019, 210: 210−231. DOI: https://doi.org/10.1016/j.conbuildmat.2019.03.099.

[23] MAHDIKHANI M, BAMSHAD O, FALLAH SHIRVANI M. Mechanical properties and durability of concrete specimens containing nano silica in sulfuric acid rain condition [J]. Construction and Building Materials, 2018. 167: 929−935. DOI: https://doi.org/10.1016/j.conbuildmat. 2018.01.137.

[24] BIRICIK H, SARIER N. Comparative study of the characteristics of nano silica-, silica fume-and fly ash-incorporated cement mortars [J]. Materials Research, 2014, 17(3): 570−582. DOI: https://doi.org/10.1590/S1516-14392014005000054

[25] QUERCIA BIANCHI G. Application of nano-silica in concrete [D]. Eindhoven: Technische Universiteit Eindhoven, 2014. DOI: https://doi.org/10.6100/IR780551.

[26] ASSI L N. Cost and fuel usage optimization of activating solution based silica fume geopolymer concrete [D]. University of South Carolina. 2017.

[27] HENDI A, RAHMANI H, MOSTOFINEJAD D, TAVAKOLINIA A, KHOSRAVI M. Simultaneous effects of microsilica and nanosilica on self-consolidating concrete in a sulfuric acid medium [J]. Construction and Building Materials, 2017, 152: 192−205. DOI: https://doi.org/10.1016/ j.conbuildmat.2017.06.165.

[28] MAHMOUD M, BASSUONI M T. Response of concrete to incremental aggression of sulfuric acid [J]. Journal of Testing and Evaluation, 2020, 48(4): 19. DOI: https://doi.org/ 10.1520/JTE20180114.

[29] HEWAYDE E, ALLOUCHE E, NAKHLA G. Experimental investigations of the effect of selected admixtures on the resistance of concrete to sulfuric acid attack [C]// Pipeline Engineering and Construction International Conference. Baltimore, Maryland, United States, 2003. DOI: https://doi.org/ 10.1061/ 40690(2003)33.

[30] RAHMANI H, RAMAZANIANPOUR A, PARHIZKAR T, HILLEMEIER B. Contradictory effects of silica fume concretes in sulfuric acid environments [C]// 3rd International Conference on Concrete & Development. Tehran, Iran, 2009: 761−774.

[31] WAFA F. Accelerated sulfate attack on concrete in a hot climate [J]. Cement, Concrete and Aggregates, 1994, 16(1): 31−35. DOI: https://doi.org/10.1520/CCA10558J.

[32] ATTIOGBE E K, RIZKALLA S H. Response of concrete to sulfuric acid attack [J]. ACI Materials Journal, 1988, 85(6): 481−488.

[33] TOKYAY M. Cement and concrete mineral admixtures [M]. Boca Raton, Florida: CRC Press, 2016.

[34] ACI COMMITTEE, 506R-16: Guide to Shotcrete [R]. Farmington Hills, MI, United States: American Concrete Institute, 2016.

[35] BERRA M, CARASSITI F, MANGIALARDI T, PAOLINI A E, SEBASTIANI M. Effects of nanosilica addition on workability and compressive strength of Portland cement pastes [J]. Construction and Building Materials, 2012, 35: 666−675. DOI: https://doi.org/10.1016/j.conbuildmat.2012. 04.132.

[36] SIDDIQUE R. Utilization of silica fume in concrete: Review of hardened properties [J]. Resources, Conservation and Recycling, 2011, 55(11): 923−932. DOI: https://doi.org/ 10.1016/j.resconrec.2011.06.012.

[37] KHALOO A, MOBINI M H, HOSSEINI P. Influence of different types of nano-SiO_2 particles on properties of high-performance concrete [J]. Construction and Building Materials, 2016, 113: 188−201. DOI: https://doi.org/ 10.1016/j.conbuildmat.2016.03.041.

[38] WONG H S, ABDUL RAZAK H. Efficiency of calcined kaolin and silica fume as cement replacement material for strength performance [J]. Cement and Concrete Research, 2005, 35(4): 696−702. DOI: https://doi.org/10.1016/ j.cemconres.2004.05.051.

[39] ASTM C192/C192M-16a. Standard practice for making and curing concrete test specimens in the laboratory [S]. West Conshohocken, PA. United States: ASTM International, 2016.

[40] ASTM C642-13. Standard test method for density, absorption, and voids in hardened concrete [S]. West Conshohocken, PA. United States: ASTM International, 2013. DOI: 10.1520/c0642-13.

[41] ASTM C39/C39M−18. Standard test method for compressive strength of cylindrical concrete specimens [S]. West Conshohocken, PA. United States: ASTM International, 2018.

[42] HOSSAIN M M, KARIM M R, HASAN M, HOSSAIN M K, ZAIN M F M. Durability of mortar and concrete made up of pozzolans as a partial replacement of cement: A review [J]. Construction and Building Materials, 2016, 116: 128−140. DOI: 10.1016/j.conbuildmat.2016.04.147.

[43] WANG J, NIU D, DING S, MI Z, LUO D. Microstructure, permeability and mechanical properties of accelerated shotcrete at different curing age [J]. Construction and Building Materials, 2015, 78: 203−216. DOI: 10.1016/ j.conbuildmat.2014.12.111.

[44] SUPIT S W M, SHAIKH F U A. Durability properties of high volume fly ash concrete containing nano-silica [J].

Materials and Structures, 2015, 48(8): 2431−2445. DOI: https://doi.org/10.1617/s11527-014-0329-0.

[45] POON C S, KOU S C, LAM L. Compressive strength, chloride diffusivity and pore structure of high performance metakaolin and silica fume concrete [J]. Construction and Building Materials, 2006, 20(10): 858−865. DOI: https://doi.org/10.1016/j.conbuildmat.2005.07.001.

[46] ABBASS W, KHAN M I, MOURAD S. Experimentation and predictive models for properties of concrete added with active and inactive SiO_2 fillers [J]. Materials, 2019, 12(2): 299. DOI: https://doi.org/10.3390/ma12020299.

[47] YAJUN J, CAHYADI J H. Simulation of silica fume blended cement hydration [J]. Materials and Structures, 2004, 37(6): 397−404. DOI: 10.1007/BF02479636.

[48] RUPASINGHE M, SAN NICOLAS R, MENDIS P, SOFI M, NGO T. Investigation of strength and hydration characteristics in nano-silica incorporated cement paste [J]. Cement and Concrete Composites, 2017, 80: 17−30. DOI: https://doi.org/10.1016/j.cemconcomp.2017.02.011.

[49] DODSON V H. Pozzolans and the pozzolanic reaction [M]// Concrete Admixtures. Boston, MA: Springer US,1990. DOI: 10.1007/978-1-4757-4843-7_7.

[50] RICHARDSON I G. The nature of C-S-H in hardened cements [J]. Cement and Concrete Research, 1999, 29(8): 1131−1147. DOI: https://doi.org/10.1016/S0008-8846(99)00168-4.

[51] BASSUONI M T, NEHDI M L. Resistance of self-consolidating concrete to sulfuric acid attack with consecutive pH reduction [J]. Cement and Concrete Research, 2007, 37(7): 1070−1084. DOI: https://doi.org/10.1016/j.cemconres.2007.04.014.

[52] PELISSER F, GLEIZE P J P, MIKOWSKI A. Effect of the Ca/Si molar ratio on the micro/nanomechanical properties of synthetic C-S-H measured by nanoindentation [J]. The Journal of Physical Chemistry C, 2012, 116(32): 17219−17227. DOI: 10.1021/jp302240c.

[53] BAHAFID S, GHABEZLOO S, DUC M, FAURE P, SULEM J. Effect of the hydration temperature on the microstructure of Class G cement: C-S-H composition and density [J]. Cement and Concrete Research, 2017, 95: 270−281. DOI: https://doi.org/10.1016/j.cemconres.2017.02.008.

[54] TORII K, KAWAMURA M. Pore structure and chloride ion permeability of mortars containing silica fume [J]. Cement and Concrete Composites, 1994, 16(4): 279−286. DOI: https://doi.org/10.1016/0958-9465(94)90040-X.

[55] MEHTA P K, MONTEIRO P J. Concrete microstructure, properties and materials [M]. New York: McGraw-Hill Education, 2014.

[56] QUERCIA G, SPIESZ P, HÜSKEN G, BROUWERS H. SCC modification by use of amorphous nano-silica [J]. Cement and Concrete Composites, 2014, 45: 69−81. DOI: https://doi.org/10.1016/j.cemconcomp.2013.09.001.

[57] ZHANG M H, ISLAM J, PEETHAMPARAN S. Use of nano-silica to increase early strength and reduce setting time of concretes with high volumes of slag [J]. Cement and Concrete Composites, 2012, 34(5): 650−662. DOI: https://doi.org/10.1016/j.cemconcomp.2012.02.005.

[58] YAJUUN J, CAHYADI J. Investigation on microstructure of silica fume cement pastes [J]. WIT Transactions on the Built Environment, 2002, 59: 221−229.

[59] LI H, YAN D, CHEN G, XU S, LIU J, HU Y. Porosity, pore size distribution and chloride permeability of shotcrete modified with nano particles at early age [J]. Journal of Wuhan University of Technology-Mater Sci Ed, 2016, 31(3): 582−589. DOI: https://doi.org/10.1007/s11595-016- 1413-9.

[60] WU Z, SHI C, KHAYAT K H, WAN S. Effects of different nanomaterials on hardening and performance of ultra-high strength concrete (UHSC) [J]. Cement and Concrete Composites, 2016, 70: 24−34. DOI: https://doi.org/10.1016/j.cemconcomp.2016.03.003.

[61] JALAL M, POULADKHAN A, HARANDI O F, JAFARI D. Comparative study on effects of class F fly ash, nano silica and silica fume on properties of high performance self compacting concrete [J]. Construction and Building Materials, 2015, 94: 90−104. DOI: https://doi.org/10.1016/j.conbuildmat.2015.07.001.

[62] KONG D, DU X, WEI S, ZHANG H, YANG Y, SHAH S P. Influence of nano-silica agglomeration on microstructure and properties of the hardened cement-based materials [J]. Construction and Building Materials, 2012, 37: 707−715. DOI: https://doi.org/10.1016/j.conbuildmat.2012.08.006.

[63] FOROOD T I, REDAELLI E, LOLLINI F, LI W, BERTOLINI L. Effects of nanosilica on compressive strength and durability properties of concrete with different water to binder ratios [J]. Advances in Materials Science and Engineering, 2016: 8453567. DOI: https://doi.org/10.1155/2016/8453567.

[64] LIM S, MONDAL P. Effects of incorporating nanosilica on carbonation of cement paste [J]. Journal of Materials Science, 2015, 50(10): 3531−3540. DOI: https://doi.org/10.1007/s10853-015-8910-7.

[65] SARGENT P. The development of alkali-activated mixtures for soil stabilisation [M]// Handbook of alkali-activated cements, mortars and concretes. Elsevier, 2015. DOI: https://doi.org/10.1533/9781782422884.4.555.

[66] ABID K, GHOLAMI R, ELOCHUKWU H, MOSTOFI M, BING C H, MUKTADIR G. A methodology to improve nanosilica based cements used in CO_2 sequestration sites [J]. Petroleum, 2018, 4(2): 198−208. DOI: https://doi.org/10.1016/j.petlm.2017.10.005.

[67] DU H, DU S, LIU X. Durability performances of concrete with nano-silica [J]. Construction and Building Materials, 2014, 73: 705−712. DOI: https://doi.org/10.1016/j.conbuildmat.2014.10.014.

[68] AYDıN A C, NASL V J, KOTAN T. The synergic influence of nano-silica and carbon nano tube on self-compacting concrete [J]. Journal of Building Engineering, 2018, 20: 467−475. DOI: https://doi.org/10.1016/j.jobe.2018.08.013.

[69] SADRMOMTAZI A, FASIHI A, BALALAEI F, HAGHI A. Investigation of mechanical and physical properties of mortars containing silica fume and nano-SiO_2 [C]// Proceedings of the Third International Conference on Concrete and Development. Tehran, Iran, 2009: 27−29.

[70] DYER T. Influence of cement type on resistance to attack from two carboxylic acids [J]. Cement and Concrete Composites, 2017, 83: 20−35. DOI: https://doi.org/10.1016/j.cemconcomp.2017.07.004.

[71] WU Lin-ping, HUANG Guang-ping, HU Chao-shi, LIU Wei Victor. Effects of cellulose nanocrystals on improving the acid resistance of cementitious composites in mining [J]. International Journal of Minerals, Metallurgy and Materials, 2020. DOI: 10.1007/s12613-020-2087-z.

[72] MAKHLOUFI Z, BEDERINA M, BOUHICHA M, KADRI E H. Effect of mineral admixtures on resistance to sulfuric acid solution of mortars with quaternary binders [J]. Physics Procedia, 2014, 55: 329−335. DOI: https://doi.org/10.1016/j.phpro.2014.07.048.

[73] RAHMANI H, RAMZANIANPOUR A. Effect of silica fume and natural pozzolanas on sulfuric acid resistance of dense concretes [J]. Asian Journal of Civil Engineering, 2008, 9(3): 303−319.

[74] FENG J, SUN J, YAN P. The influence of ground fly ash on cement hydration and mechanical property of mortar [J]. Advances in Civil Engineering, 2018. DOI: https://doi.org/10.1155/2018/4023178.

[75] AL-SWAIDANI A M, ALIYAN S D, ADARNALY N. Mechanical strength development of mortars containing volcanic scoria-based binders with different fineness [J]. Engineering Science and Technology, 2016, 19(2): 970−979. DOI: https://doi.org/10.1016/j.jestch.2015.12.006.

[76] TSUBONE K, YAMAGUCHI Y, OGAWA Y, KAWAI K. Deterioration of concrete immersed in sulfuric acid for a long term [J]. Key Engineering Materials, 2016, 711: 659−664. DOI: https://doi.org/10.4028/www.scientific.net/KEM.711.659.

[77] HUANG Cheng-yi, FELDMAN R F. Hydration reactions in portland cement-silica fume blends [J]. Cement and Concrete Research, 1985, 15(4): 585−592. DOI: https://doi.org/10.1016/0008-8846(85)90056-0.

[78] KADRI E H, KENAI S, EZZIANE K, SIDDIQUE R, de SCHUTTER G. Influence of metakaolin and silica fume on the heat of hydration and compressive strength development of mortar [J]. Applied Clay Science, 2011, 53(4): 704−708. DOI: https://doi.org/10.1016/j.clay.2011.06.008.

[79] SIAD H, LACHEMI M, SAHMARAN M, HOSSAIN K M A. Effect of glass powder on sulfuric acid resistance of cementitious materials [J]. Construction and Building Materials, 2016, 113: 163−173. DOI: https://doi.org/10.1016/j.conbuildmat.2016.03.049.

[80] NEMATZADEH M, FALLAH-VALUKOLAEE S. Erosion resistance of high-strength concrete containing forta-ferro fibers against sulfuric acid attack with an optimum design [J]. Construction and Building Materials, 2017, 154: 675−686. DOI: https://doi.org/10.1016/j.conbuildmat.2017.07.180.

[81] LESLIE J, CHEESMAN W. An ultrasonic method of studying deterioration and cracking in concrete structures [J]. Journal of the American Concrete Institute, 1949, 21(1): 17−36.

[82] FELDMAN R F. Non-destructive testing of concrete [J]. Canadian Building Digest, 1977, 187: 4.

[83] KHAN H A, CASTEL A, KHAN M S H, MAHMOOD A H. Durability of calcium aluminate and sulphate resistant Portland cement based mortars in aggressive sewer environment and sulphuric acid [J]. Cement and Concrete Research, 2019, 124: 105852. DOI: https://doi.org/10.1016/j.cemconres.2019.105852.

[84] GRANDCLERC A, DANGLA P, GUEGUEN-MINERBE M, CHAUSSADENT T. Modelling of the sulfuric acid attack on different types of cementitious materials [J]. Cement and Concrete Research, 2018, 105: 126−133. DOI: https://doi.org/10.1016/j.cemconres.2018.01.014.

[85] GU L, BENNETT T, VISINTIN P. Sulphuric acid exposure of conventional concrete and alkali-activated concrete: Assessment of test methodologies [J]. Construction and Building Materials, 2019, 197: 681−692. DOI: https://doi.org/10.1016/j.conbuildmat.2018.11.166.

(Edited by HE Yun-bin)

中文导读

硅粉与纳米硅粉水泥基材料的耐酸性

摘要：为了研究硅粉与纳米硅粉作为添加剂对水泥砂浆耐酸性的影响，本文将标准养护后的样品浸泡于 pH=2 的硫酸溶液中，并分析了样品在浸泡实验前后的性能变化。实验结果表明，添加硅粉及纳米硅粉能有效提高浸泡前水泥砂浆的单轴抗压强度，降低可渗透孔隙的体积率。相较于纳米硅粉，硅粉对水泥砂浆的性能影响更为显著。在硫酸溶液中浸泡 75 d 后，样品出现了不同程度的腐蚀。其中，掺 5%硅粉及 1%纳米硅粉的样品展现了最低的质量损失及长度损失。

关键词：耐酸性；纳米硅粉；硅粉；水泥砂浆